

ATMOSPHERIC TELECONNECTIONS FOR ANNUAL MAXIMUM ICE COVER ON THE LAURENTIAN GREAT LAKES

RAYMOND ASSEL^{a,*} and SERGEI RODIONOV^b

^a *National Oceanic and Atmospheric Administration, Great Lakes Environmental Research Laboratory, 2205 Commonwealth Blvd, Ann Arbor, MI 48105-2945, USA*

^b *University of Colorado, Computer Science Department, Engineering Center, ECOT 7-15, Campus Box 430, Boulder, CO 80309-0430, USA*

ABSTRACT

Great Lake ice cover records for winters 1963–1990 were used to define anomalously high (low) average ice cover based on the seven highest (seven lowest) annual maximum ice covers. Analysis of the maximum ice cover reveals (i) a low (1964–1976); (ii) a high (1977–1982); and (iii) once again a low (1983–1990) ice cover regime. The high ice cover regime corresponded in part with a hiatus in El Niño–Southern Oscillation (ENSO) events and the beginning of an interdecadal change in Northern Hemisphere atmospheric circulation that started in the late 1970s. About 46% of the lowest quartile ice covers occurred during the mature phase (year + one winter) of El Niño. Only 1 year out of seven with the mature phase of El Niño between 1963 and 1990 was not associated with the lowest quartile ice cover, this was 1977, a pivotal year after which a new climatic regime in the Northern Hemisphere was established. Anomaly maps of 700 hPa geopotential height for the lowest quartile ice cover reveal a zonal flow pattern. Highest quartile ice cover was associated with meridonal circulation from the Arctic directed toward the Great Lakes. Significant differences occur for highest minus lowest quartile ice cover composite 700 hPa height anomaly maps in the Pacific Ocean, the west coast of North America, north Mexico, eastern North America, north central Siberia, western Europe and the adjacent North Atlantic. Correlations between first differences (year $t + 1$ minus year t) of annual maximum ice cover and 700 hPa geopotential heights for winters 1963–1990 agrees with these teleconnections and were higher than the absolute time series correlations, indicating strong interannual teleconnections. Annual maximum ice cover was also significantly correlated with the tropical Northern Hemisphere teleconnection index. © 1998 Royal Meteorological Society.

KEY WORDS: Laurentian Great Lakes; teleconnections; lake ice; North America; 700 hPa Northern Hemisphere anomalies; ENSO

1. INTRODUCTION

The Laurentian Great Lakes, located in the mid-latitude of eastern North America (Figure 1) contain about 95% of the USAs' and 20% of the world's fresh surface water supply. Nearly one-eighth of the population of the USA and one-third of the population of Canada live within their drainage basin. This area is very sensitive, socially and economically, to factors that affect the Great Lakes. The ice cover that forms on the Laurentian Great Lakes each winter affects the regional economy (Niimi, 1982) and the Lake's ecosystem (Vanderploeg *et al.*, 1992; Brown *et al.*, 1993; Magnuson *et al.*, 1995). The ice cover is also a sensitive indicator of regional climate and climate change (Smith, 1991; Hanson *et al.*, 1992; Ryan *et al.*, 1994; Assel and Robertson, 1995). Several studies over the past two decades (Assel and Quinn, 1979; Assel *et al.*, 1985; Assel, 1987) provide evidence that anomalous ice cover (much above or much below average) occurs on the Great Lakes during ENSO events. A more recent study (Assel, 1992) demonstrated that there is a high correlation (0.93) between a 20-winter average (1960–1979) of the monthly cumulative value of the Pacific North America (PNA) index (December through to April) and a 20-winter average of monthly ice cover. That study also showed that there is an equally high correlation

* Correspondence to: National Oceanic and Atmospheric Administration, Great Lakes Environmental Research Laboratory, 2205 Commonwealth Blvd, Ann Arbor, MI 48105-2945, USA. E-mail: assel@glerl.noaa.gov

Contract grant sponsor: Great Lakes Environmental Research Laboratory; Contract grant number: 1020

(0.93) between the departure of the 1990 monthly average ice cover from a 20-year average with the departure of the cumulative value of the PNA index from its 20-year average. These results provide the motivation for this present work. The objective of the current study is to develop an improved understanding of Great Lakes ice cover teleconnections that may lead to follow-up studies with applications to first model and then develop improved methods to forecast seasonal ice cover for the Great Lakes. Here the annual maximum values of ice coverage over a 28-winter period (1963–1990) for each Great Lake is examined with respect to changes in its mean value over the three decades and its relation to ENSO events. Northern Hemisphere circulation anomalies associated with anomalously high and low annual maximum ice cover and teleconnections of ice cover with the northern Hemisphere 700 hPA geopotential field are also examined.

2. DATA AND ANALYSIS METHODS

2.1. Annual maximum ice cover

Systematic lake-scale observations of Great Lakes ice cover began in the 1960s by Federal agencies in the USA (US Army Corps of Engineers, US Coast Guard) and Canada (Atmospheric Environment Service, Canadian Coast Guard) to support early and late season navigation, the closing of the navigation season in winter, and the opening of navigation in spring. Observations were made at irregular intervals primarily to support operational activities. Ice charts depicting ice concentration patterns and ice extent were constructed from satellite imagery, side-looking airborne radar imagery, and visual aerial ice reconnaissance. Estimates of the annual maximum ice extent, that is the greatest per cent of surface area of a lake covered by ice each winter for each Great Lake, for most winters were abstracted from published reports: DeWitt *et al.* (1980), Assel (1986a, 1987, 1989, 1992). Annual maximum ice cover for winters, 1984, 1985, 1988, 1989 were estimated using an electronic digitizer and ice charts produced by the US Department of Commerce, National Oceanic and Atmospheric Administration and by the Atmospheric Environment Service in Canada (available from the National Snow and Ice Data Center, User Services, CIRES, Campus Box 449, University of Colorado, Boulder CO 80309-0449, USA). In this analysis the upper and lower 25% of the distribution of annual maximum ice cover for each Great Lake were used to

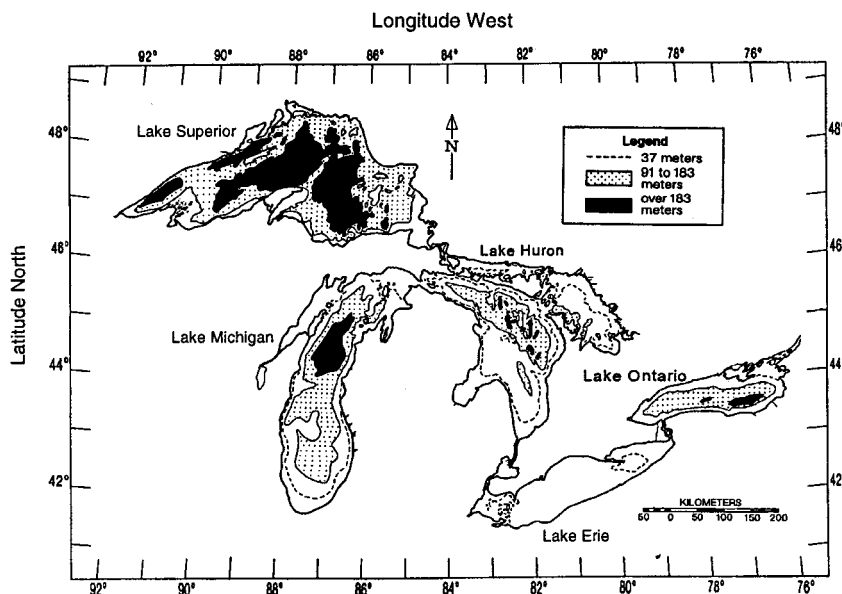


Figure 1. Great Lakes bathymetry

identify winters with anomalously high and low ice cover. Because many scientists believe that relationships between climatic variables become more clear for extreme values, the quartile criterion was chosen as a compromise between our desire to better separate positive and negative anomalies in ice cover and the number of observations in each group.

2.2. 700 hPa geopotential heights

The 700 hPa heights data set used in this study is the National Meteorological Center's Northern Hemisphere monthly grided data set, see Jenne (1975), and National Center for Atmospheric Research (1996) for a description and availability. Average (DJF) 700 hPa geopotential heights were calculated for each winter: 1963 (December 1962, January 1963, February 1963), 1964 (December 1963, January 1964, February 1964), and so on to 1990 (December 1989, January 1990, February 1990). These winter averages for the 7 years of the highest quartile ice cover for each Great Lake were used to calculate the composite maps for the high ice cover winters, and similarly for the lowest quartile ice cover winters at each Great Lake. Anomalies were calculated as deviations from the 28-winter mean 700 hPa (DJF) geopotential height for the period 1963–1990. Correlations of annual maximum ice cover for each Great Lake for all Northern Hemisphere grid-points of the winter average 700 hPa height fields were also made in order to identify teleconnections.

2.3. Atmospheric circulation patterns

Circulation pattern characteristics reminiscent of the North Atlantic Oscillation (NAO), the PNA, and the Tropical Northern Hemisphere (TNH) teleconnection patterns appear in 700 hPa composite anomaly maps and 700 hPa composite anomaly difference maps for winters with the lowest and highest annual maximum ice cover and in correlation maps of annual maximum ice cover with average winter 700 hPa geopotential heights. Descriptions of these three teleconnection patterns are not given here for the sake of brevity but are available elsewhere (e.g. van Loon and Rogers, 1978; Wallace and Gutzler, 1981; Mo and Livezey, 1986; Barnston and Livezey, 1987). The indices of the NAO, PNA, and TNH used in this study are available from the Climate Diagnostic Center (NOAA) and are regularly published in the *Climate Diagnostics Bulletin*. In this study, mean winter values for these three indices were correlated with annual maximum ice cover. Mean winter indices were derived from monthly values of these indices averaged for 3 months: December, January, and February for the NAO and PNA indices. As there were no February data for the TNH index, the averaging procedure in this case was applied only for 2 months: December and January.

3. GREAT LAKES ANNUAL MAXIMUM ICE COVER REGIME

The Great Lakes do not freeze-over completely because of their large heat storage capacity, large surface areas, and the action of winds. Annual maximum ice cover varies from less than 30% (Assel *et al.*, 1985) to over 90% (Assel *et al.*, 1996). Differences in *annual maximum ice cover anomalies* among the Great Lakes for a given winter are attributable to differences in the timing, duration, intensity, and frequency of: episodic high winds, anomalous calm, and cold periods over each lake. The effects of a given cold air outbreak, calm period, or storm can affect some or all of the Great Lakes and the effects of the same forcing can vary from year to year depending upon pre-existing ice cover and lake heat storage.

Differences in *the long-term (1963–1990) average* annual maximum ice cover extent among the Great Lakes are due primarily to differences in lake heat-storage capacity and winter air temperatures. The former relates to lake bathymetry patterns (Figure 1) and mean lake depth (Table I) and the latter to the general decrease of air temperatures with increase in latitude. Lake Erie, southernmost of the Great Lakes, is exposed to the mildest air temperatures; it develops the largest ice cover because it has the smallest mean depth (Table I). Lake Superior has the largest mean depth but second-largest ice cover due to its northernmost location and thus lowest air temperatures. Lake Superior's ice cover is correlated most

Table I. Summary of Great Lakes physical features, seasonal maximum freezing degree-days (FDD), and ice cover

	Superior	Michigan	Huron	Erie	Ontario
Depth (m) ^a	148	85	59	19	86
Area ^b	82	58	59	26	19
FDD (°C) ^c	928	447	572	216	324
Ice (%) ^d	69	37	64	90	25

^a Mean lake depth (lake volume divided by surface area).

^b Lake surface area rounded to nearest 1000 km².

^c Normal annual maximum FDD given in Assel (1986b).

^d Average of annual maximum ice cover for winters 1963–1990.

Table II. Correlation coefficients^a of annual maximum ice cover among the Great Lakes

Latitude	(°N)	Superior	Michigan	Huron	Ontario	Erie
47.75	Superior	*				
44.00	Michigan	0.65	*			
44.50	Huron	0.74	0.79	*		
43.50	Ontario	0.48	0.81	0.76	*	
42.13	Erie	0.53	0.37	0.47	0.36	*

^a Rounded to the nearest hundredth.

highly with lakes most similar in latitude, Michigan and Huron (Table II). Lakes Michigan, Huron, and Ontario, with water masses between 43°N and 46°N, have highest ice cover decreases as the mean depth increases for these three Great Lakes (Table I). Lake Michigan's ice cover exceeds Lake Ontario's, despite a similar mean depth, because it (Lake Michigan) is farther north and has shallow areas in its northern section.

The 28-winter series of annual maximum ice cover has a temporal pattern of low–high–low. During the winters 1963–1976, 71% of the lowest quartile ice covers occurred; during the winters 1977–1982, 66% of the highest quartile ice covers occurred; and during the winters 1983–1990, 20% of the lowest quartile ice covers occurred. This distribution of the extreme winters is given in Table III, and the mean value for each of the three periods is given as Table IV. A two-tailed *t*-test of mean ice cover for each Great Lake for each of the three periods indicates that the mean for winters 1977–1982 is significantly different (at the 5% level) from the means of either of the other two periods, and that the means of annual maximum ice cover for the other two periods do not differ significantly from each other. These trends may be related to the occurrence of ENSO events and changes in large-scale atmospheric circulation patterns over that 28-year period.

4. ENSO EVENT—ANNUAL MAXIMUM ICE COVER COMPARISONS

Numerous studies have shown that ENSO events are related to winter temperature anomalies (and thus possibly to Great Lakes ice cover) in North America (e.g. Kiladis and Diaz, 1989; Ropelewski and Halpert, 1986). Here, a preliminary and exploratory comparison is made between Great Lakes annual maximum ice cover and the occurrence of ENSO events. No attempt is made to derive statistical significance to the results because of the qualitative nature of the analysis and limited amount of data. In this study, an ENSO event is defined (after Kiladis and Diaz, 1989) to start when the following three events occur: (i) tropical Pacific sea-surface temperature (SST) is positive for three seasons; (ii) SST is at least 0.5°C greater than the mean for one of the three seasons; and (iii) the Southern Oscillation Index (SOI) is less than –1.0 for the three seasons. Year 0 of a warm ENSO event is the year when the SOI changes sign from positive to negative, and the central and eastern equatorial Pacific SST anomalies become strongly positive. Year 0

Table III. The distribution of the seven winters with annual maximum ice cover in the lowest quartile (O) and the seven winters with annual maximum ice cover in the highest quartile (X) of the 28-winter period 1963–1990 and ancillary data on ENSO events

Year	Lake					Year	ENSO (Kiladis and Diaz, 1989)	Comments
	Superior	Michigan	Huron	Erie	Ontario			
1963	X	X	X	—	X	1963	Warm	Winters 1964–1976 tile had the greatest frequency of lowest quartile ice cover; a majority of the ENSO events also occurred during these 13 winters.
1964	O	O	O	—	—	1964	Cold	
1965	—	—	—	O	O	1965	Warm	
1966	—	O	O	O	—	1966		
1967	—	X	X	—	O	1967		
1968	X	—	—	—	O	1968		
1969	O	O	O	O	O	1969	Warm	
1970	—	—	—	—	—	1970	Cold	
1971	O	—	O	—	O	1971		
1972	X	X	—	—	—	1972	Warm	
1973	—	O	—	—	—	1973	Cold	
1974	—	O	—	—	—	1974	Cold	
1975	O	—	O	O	—	1975	Cold	
1976	O	O	—	—	—	1976	Warm	
1977	—	X	X	X	X	1977		Winters 1977–1982 had the greatest frequency of highest quartile ice cover and lowest occurrence of ENSO events.
1978	—	X	X	X	X	1978		
1979	X	X	X	X	X	1979		
1980	—	—	—	—	X	1980		
1981	X	—	X	X	X	1981		
1982	X	X	X	X	X	1982	Warm	
1983	O	O	O	O	O	1983		
1984	—	—	—	—	—	1984		Winters 1983–1990 had lowest occurrence of highest quartile ice strongest ENSO events on record.
1985	—	—	—	—	—	1985		
1986	—	—	—	—	—	1986	Warm	
1987	O	—	O	O	O	1987		
1988	—	—	—	X	—	1988	Cold	
1989	X	—	—	X	—	1989		
1990	—	—	—	O	—	1990		
X	90	45	80	99	34	X	Lowest observed value ^a of highest quartile	
	70	36	64	90	25		Mean ^a for all winters between 1963 and 1990	
O	48	20	50	85	12	O	Highest observed value ^a of lowest quartile	

^a Percentage of surface area covered by ice, rounded to nearest 1%.

of a cold ENSO event is defined as having just the opposite characteristics. Cold ENSO events are also known as La Niña or anti-El Niño events.

4.1. ENSO event winters

The ENSO events in Table III are for year 0 of the ENSO cycle. Warm and cold ENSO events are compared separately (i.e. without regard to overlapping years of cold or warm ENSO events) with high and low quartile ice cover (Table V) to identify possible teleconnections. The strongest signal is seen for the year + 1 warm ENSO winters for low quartile ice cover. The reason no correspondingly strong signal is found for La Niña (cold ENSO) events winters for high quartile ice cover is unknown. The warm year + 1 ENSO winters, which comprise only 25% of all winters considered, have 46% of the lowest quartile ice cover. Five (1964, 1966, 1973, 1983, 1987) of the 7 year + 1 warm ENSO winters in Table III have at least one lake with a lowest quartile ice cover, winters 1970 and 1977 being the exceptions; and four out

Table IV. Mean of annual maximum Great Lakes ice covers^a

Lake	Winter seasons		
	1963–1976	1977–1982	1983–1990
Superior	65.85	88.16	62.37
Michigan	30.42	64.16	26.50
Huron	55.92	91.00	56.87
Erie	90.78	99.16	81.50
Ontario	17.57	51.83	18.37

^a Percentage of surface area covered by ice.

of these five mild winters (1964, 1966, 1983, 1987) have three or more of the Great Lakes in the lowest quartile of annual maximum ice cover. This is in good agreement with Kiladis and Diaz (1989) and with Ropelewski and Halpert (1986), both of whom found a relation between year + 1 warm ENSO events and above average winter temperatures for a region extending from north-western Canada to Lake Superior. The much above average ice cover during winter 1977, which is also a warm ENSO year + 1 may be associated with the interdecadal change in Northern Hemisphere atmospheric circulation that started in 1977, as noted below.

4.2. Non-ENSO event winters

Fifty-four per cent of the high quartile ice covers occurred during five consecutive winters without warm or cold ENSO events, the winters from December 1977–March 1978 to December 1981–March 1982. The lack of ENSO events in the late 1970s and early 1980s is associated with an interdecadal change in Northern Hemisphere atmospheric circulation (Trenberth, 1990) and changes in Pacific SST (tropical and extratropical North and South Pacific) that resulted in a change in the background state on which El Niño evolves (Wang, 1995). Changes included a strengthening and eastward shift of the Aleutian Low in winter, resulting in advection of warmer and moister air into Alaska and advection of colder air over the North Pacific, warming SSTs in the tropical, and cooling SSTs in the extratropical Pacific. The colder than normal SSTs in the central North Pacific accompanied by warmer than normal waters along the North American seaboard contributed to an intensification of the upper atmospheric ridge over the Rocky

Table V. Number of lowest (O) and highest (X) quartile of annual maximum ice cover occurring the year prior (–1), the year of (0), or the year after (+1) a warm or cold ENSO event and the percentage of all lowest or highest quartile ice covers for each category

Year ^a	Warm ENSO event			Year	Cold ENSO event		
	–1	0	+1		–1	0	+1
1963	—	4X	3O	1964	4X	3O	2O
1965	3O	2O	3O	1970	5O	—	3O
1969	(1O, 1X)	5O	—	1973	2X	1O	1O
1972	3O	2X	1O	1975	1O	3O	2O
1976	3O	2O	4X	1988	4O	1X	2X
1982	4X	5X	5O				
1986	—	—	4O				
X (%)	14	31	11		17	3	6
O (%)	29	25	46		29	20	23

^a The years in this table are for year 0 of the ENSO event, e.g. 1963 for the warm ENSO event is year 0 of that event, 1962 is year –1 of that event, and 1964 is year +1 of that event, and similarly for the other years listed in this table.

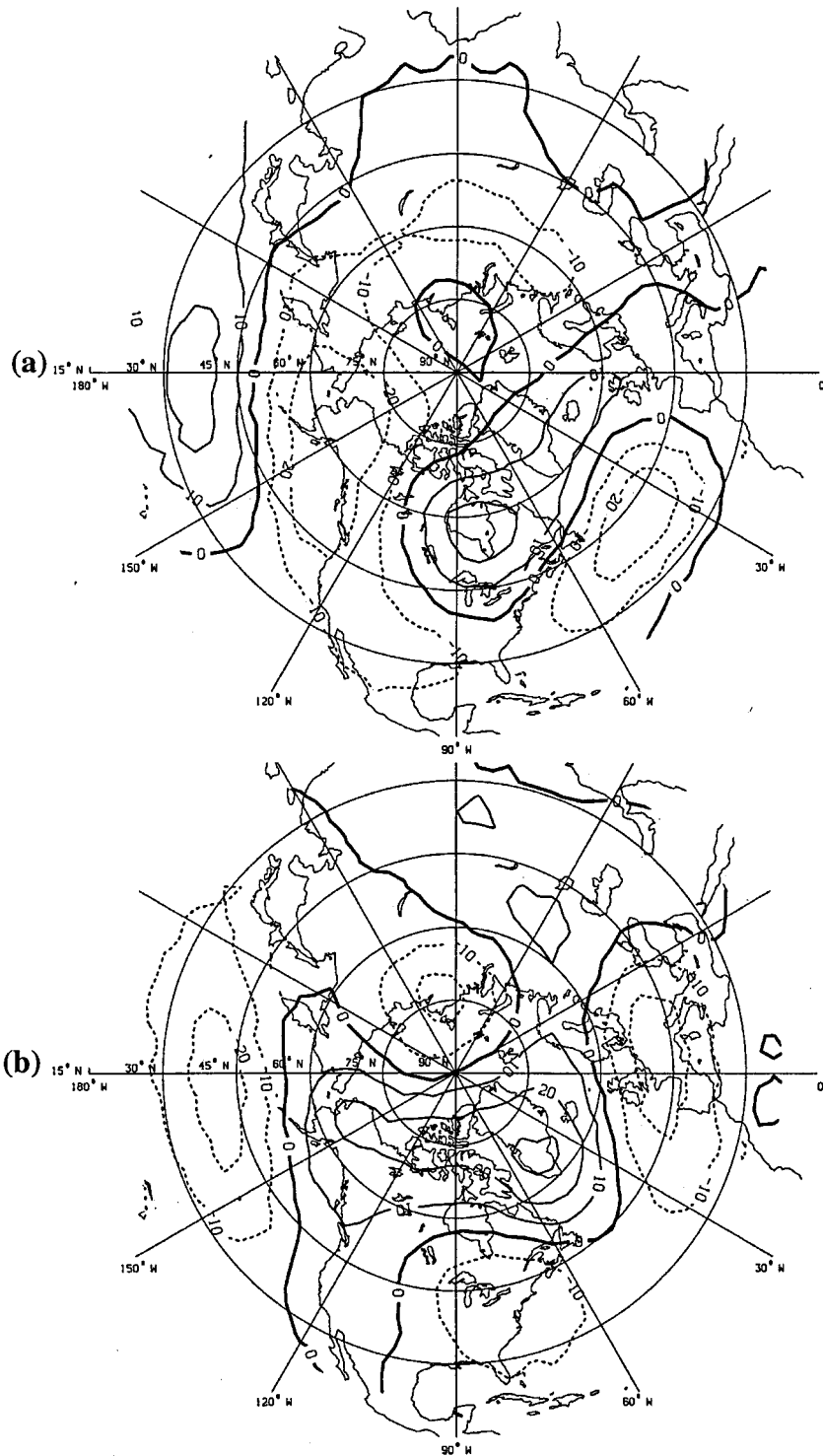


Figure 2. 700 hPa composite anomaly maps (metres) for Lake Huron (a) lowest quartile and (b) highest quartile ice cover. Dashed lines indicate negative anomaly

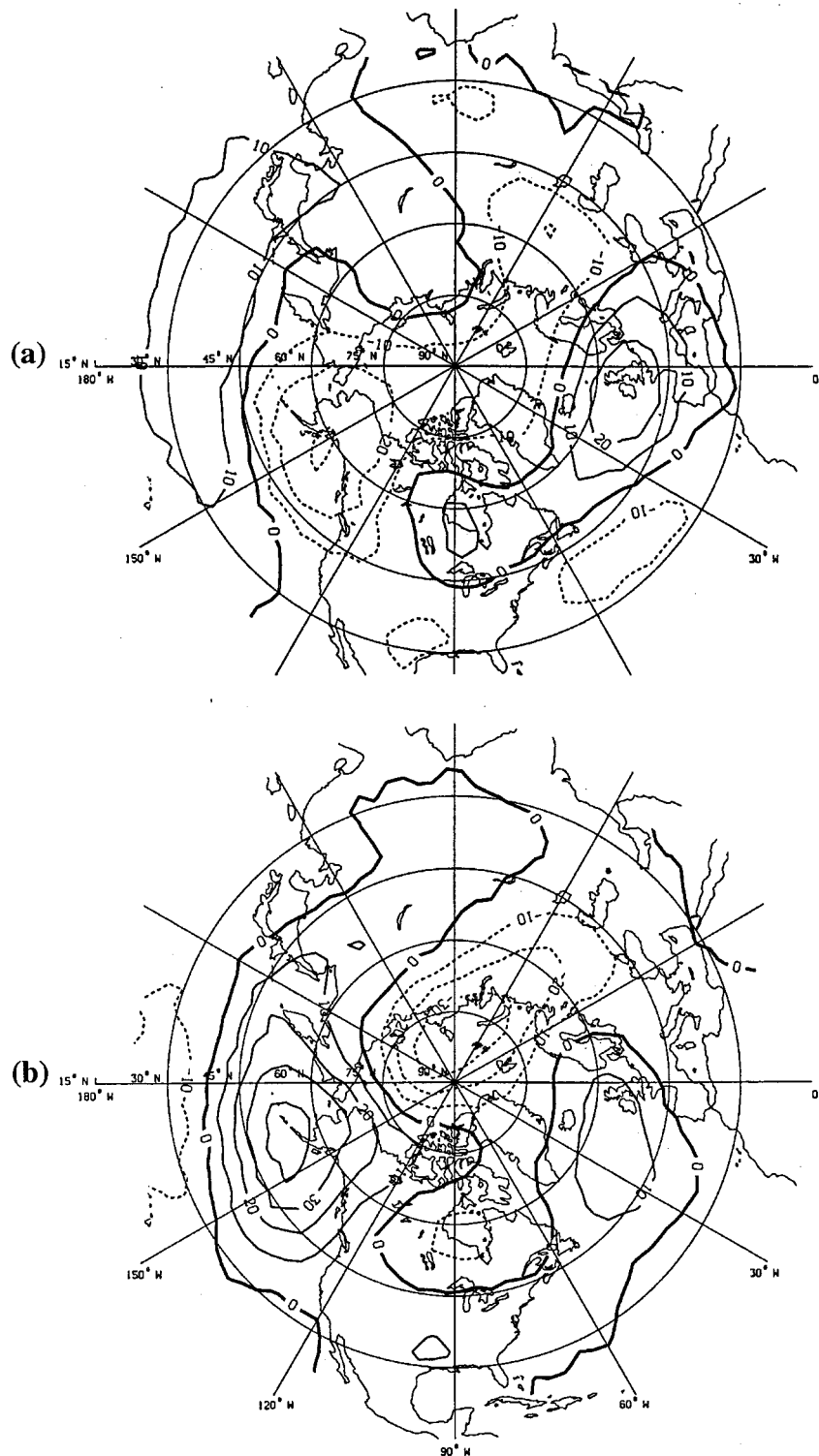


Figure 3. 700 hPa composite anomaly (metres) for Lake Superior (a) lowest quartile and (b) highest quartile ice cover. Dashed lines indicate negative anomaly

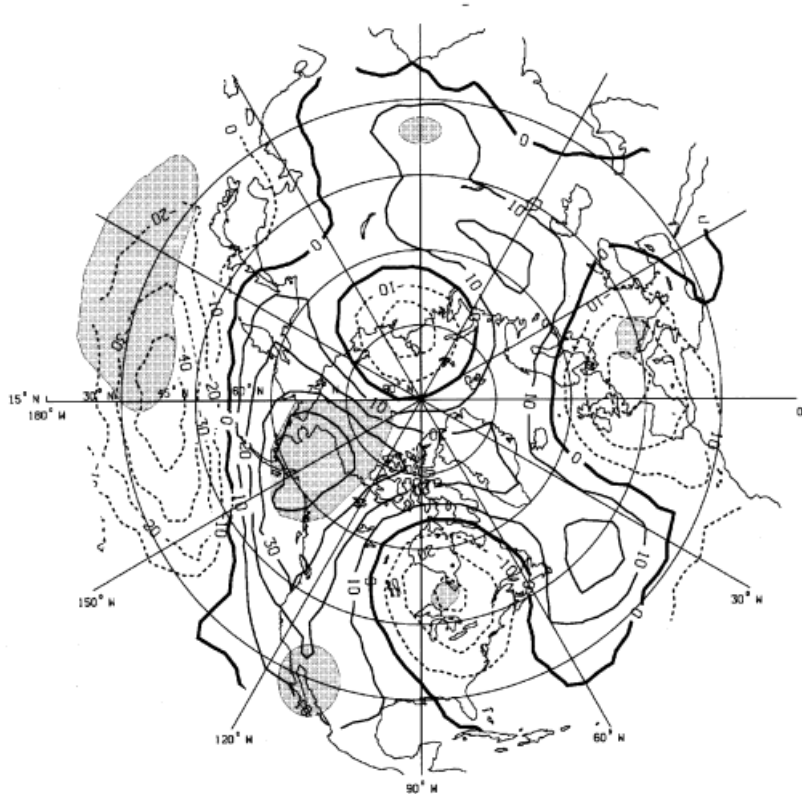


Figure 4. 700 hPa anomaly difference (for highest quartile minus lowest quartile ice cover; units are in metres) for Lake Huron. Shaded areas are significant at the 5% level, using a two-tailed Student's *t*-test. Dashed lines indicate negative anomaly differences

Mountains and trough over the eastern USA (Trenberth, 1990; Graham, 1994). These changes in the ridge–trough complex tended to direct arctic and polar air masses southward toward the middle and eastern sections of North America and resulted in a series of extremely cold winters in this region (Harnack, 1980).

In 1977, significant climatic changes were also observed in the North Atlantic sector. A new climatic regime established here in the following years was similar to that of the 1960s and was characterized by the weakening of the mid-latitude westerlies and predominantly negative NAO index (Dooley *et al.*, 1984). Unlike the North Pacific, where the climatic regime described above lasted until the late 1980s, the North Atlantic climatic regime was most extreme during the period of 1977–1982 (Rodionov and Krovnin, 1992).

5. COMPOSITE 700 hPa CIRCULATION PATTERN FOR HIGHEST AND LOWEST QUARTILE ICE COVER

The 28-year mean (1963–1990) of mean winter (December, January, February, DJF) 700 hPa geopotential heights was subtracted from the composite 700 hPa geopotential heights of the 7 years with the highest (lowest) quartile annual maximum ice cover for each Great Lake. The resultant anomaly maps portray northern hemispheric circulation anomalies for lowest and highest quartile ice cover.

5.1. Lowest quartile anomaly maps

A majority of the lowest quartile ice covers on all the lakes occurred during the winters: 1964, 1966, 1969, 1971, 1975, 1983, and 1987 (Table III). Only the map of Lake Huron is shown here for the sake of

brevity; details of the pattern vary for each Great Lake, but overall the pattern is similar. The composite map for the lowest quartile for Lake Huron (Figure 2(a)) is characterized by a wavetrain in the middle and high latitudes, with positive anomalies over the central North Pacific and to the north of the Great Lakes (a third centre is located in the North Atlantic at about 55°N, 30°W for Lake Ontario and farther east in north-west Europe for Lake Superior) and negative anomalies centred just offshore of the west coast of North America and in the mid-Atlantic. The distribution of 700 hPa anomalies implies a weakening of the quasi-permanent ridge over the west coast and a weakening of the trough over eastern North America that results in a strengthened zonal flow bringing moderate winter air temperatures to the Great Lakes. A weakening of the Baffin Island low, and to a lesser degree the Icelandic low, indicates less frequent invasion of arctic and polar air into the Great Lakes region.

5.2. Highest quartile anomaly maps

A majority of the highest quartile ice cover occurred during the winters: 1963, 1977, 1978, 1979, 1981, and 1982 (Table III). The 700 hPa composite anomaly pattern for highest quartile ice cover of Lakes Michigan, Ontario, and Erie is similar to that of Lake Huron, so for the sake of brevity only the composite map for Lake Huron (Figure 2(b)) is shown. The pattern of Lake Huron has centres of below average 700 hPa heights in the central Pacific Ocean, over and to the south-east of the Great Lakes, and over western Europe and the adjacent North Atlantic. Above average 700 hPa heights are located along the west coast of North America, and north of 50°N extend eastward from Alaska to Greenland, with the major centre of positive anomalies over southern Greenland. The combined effect of these patterns produces a strengthening of the troughs in the mid-Pacific Ocean and over the eastern third of North America and a strengthening of the ridge over the west coast of North America, resulting in a meridional flow regime with increased advection of cold arctic and polar air masses into the mid-section and eastern portion of North America. A strong ridge over western Canada during winter has often been associated with above average ice cover in the Great Lakes (Quinn *et al.*, 1978; Assel *et al.*, 1979; DeWitt *et al.*, 1980; Assel *et al.*, 1996).

5.3. Lowest and highest quartile anomaly map comparisons

The composite 700 hPa circulation patterns for lowest (Figure 2(a)) and highest (Figure 2(b)) quartile ice cover are not symmetric to each other. The 700 hPa anomaly centre in the eastern part of North America located over or to the north of the Great Lakes in Figure 2(a) is shifted south or south-east in Figure 2(b). This is the case for all lakes except Superior (Figure 3(a and b)), where the anomaly centres in the eastern part of North America are practically mirror images of each other. Another important difference of the composite anomaly maps of Figure 2(b) relative to Figure 2(a) is an absence of a positive anomaly centre in the central North Atlantic for the years of highest quartile ice cover (Figure 2(b)) similar to the strong negative anomaly centre for the years of lowest quartile ice cover (Figure 2(a)). The entire mid-latitude belt (Figure 2(b)) in this sector is occupied by negative 700 hPa anomalies with two centres, to the south-east of the Great Lakes and over western Europe. The main centre of positive anomalies for Lake Huron (Figure 2(b)) is located over southern Greenland. This anomaly circulation pattern is characteristic of a significant weakening of mid-latitude westerlies over the North Atlantic and negative temperature anomalies in north-western Europe and European Arctic seas. In fact, during all the years of the highest quartile ice cover in the Great Lakes, mean winter sea temperature of the Kola section of the Barents Sea (which serves as an acknowledged indicator of temperature regime in the entire north-east Atlantic region) exhibited negative anomalies (Rodionov and Krovvin, 1992). However, we cannot say the opposite for the years of the lowest quartile ice cover. For those years, the number of positive temperature anomalies in the Kola section was almost equal to the number of negative anomalies.

A map of the difference between the composite 700 hPa anomaly map for highest quartile minus the composite 700 hPa anomaly map for lowest quartile ice cover was constructed for each Great Lake. A two-tail Student's *t*-test was used to identify areas where anomaly differences were locally significant at the 5% level. Only the difference map for Lake Huron (Figure 4) is shown because it is representative of

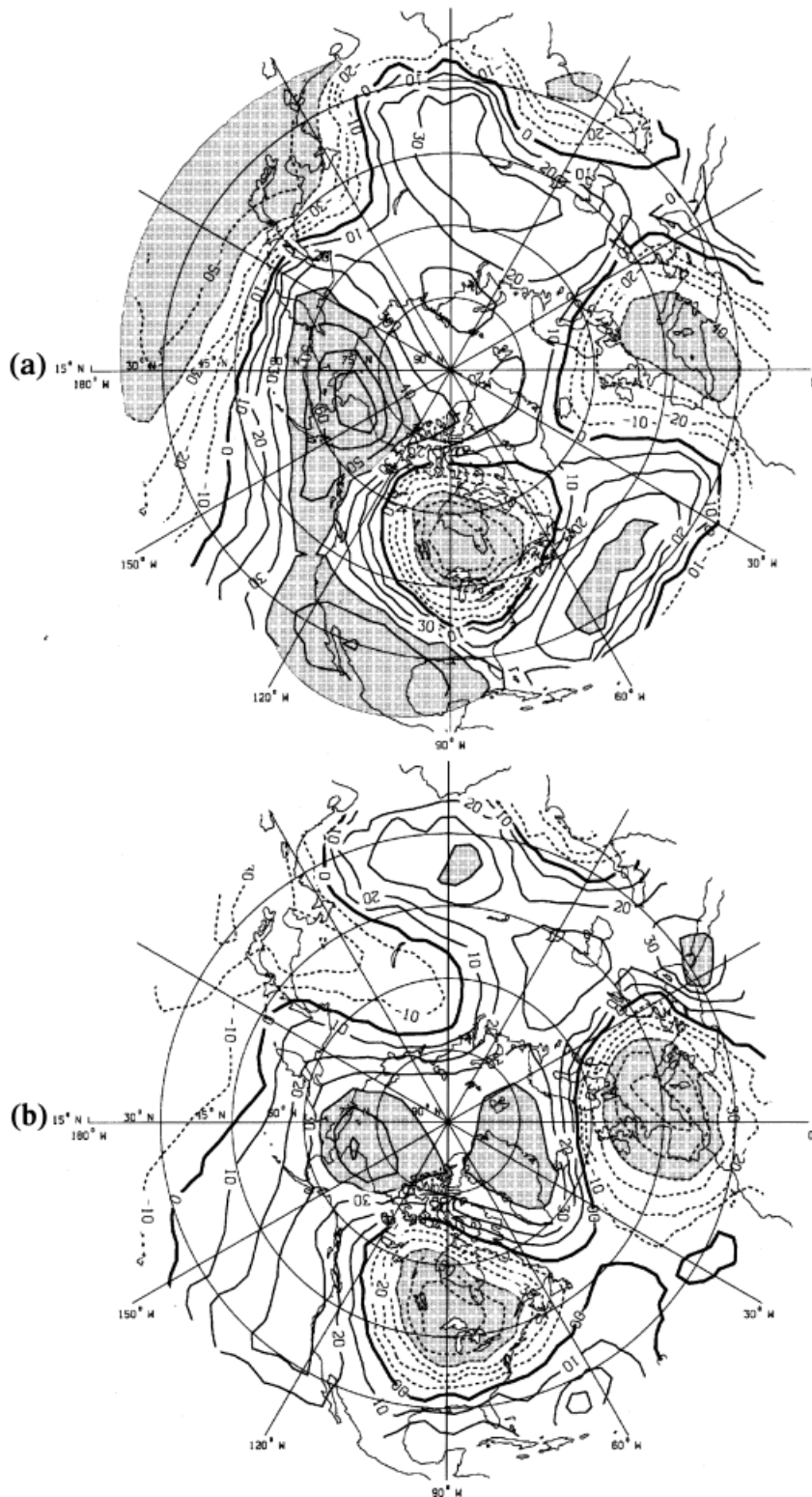


Figure 5. First difference 700 hPa annual maximum ice cover correlation coefficients ($\times 100$) (a) Lake Superior; (b) Lake Michigan; (c) Lake Huron; (d) Lake Erie; (e) Lake Ontario. Shaded areas are significant at the 5% level, using a two-tailed Student's *t*-test. Dashed lines indicate negative correlations

the Great Lakes in general. Map features for the other Great Lakes that vary from the Lake Huron difference map are described in the text. Significant negative anomaly difference centres occur in the central North Pacific, in the vicinity of the Great Lakes, in the central Atlantic (not shown in Figure 4), and in Europe; the area of negative differences for the Great Lakes is largest for Lake Michigan and smallest for Lakes Superior and Ontario. Centres of significant positive differences are located over Alaska, over northern Mexico to south-western USA, over central Asia, and (for Lake Michigan only) over the North Atlantic between Greenland and northern Norway. Further credence for these patterns is provided (below) by examining patterns of correlations of annual maximum ice cover for all 28 winters (1963–1990) with the 700 hPa geopotential height field.

6. CORRELATIONS OF ANNUAL MAXIMUM ICE COVER WITH 700 hPa GEOPOTENTIAL HEIGHTS

Statistically the presence of trend in time series to be correlated generally acts to invalidate both the assumption of being stationary and the assumption of being independent of nearby (in time) elements of each series. Thus, detrending with the first difference permits a more accurate estimate of the correlation of interest (Jenkins and Watts, 1968). Also, earlier studies (Rogers, 1976; Assel, 1990) suggest a Quasi-biennial Oscillation (QBO) pattern in the annual maximum ice cover time series. For these reasons we made correlations of the first difference of annual maximum ice cover (year $t + 1$ minus year t) with the first difference of average winter 700 hPa geopotential heights (Figure 5 (a–e)). (Correlations of the

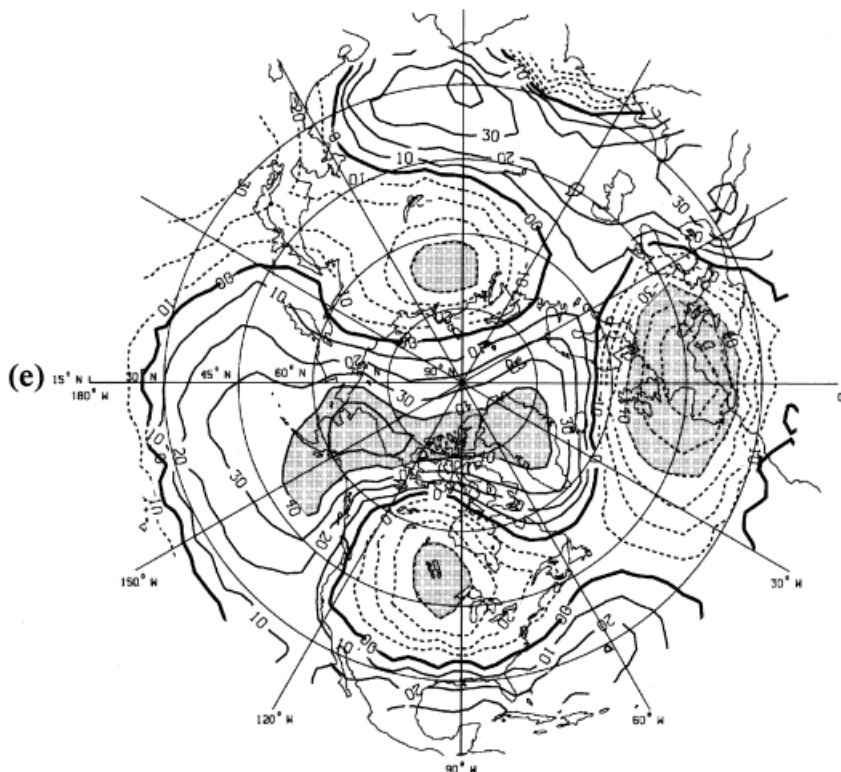


Figure 5 (Continued)

Table VI. Correlation coefficients ($\times 100$) between the NAO, PNA and TNH teleconnections indices and maximum ice cover for the original time series and their first differences (numbers in italic indicate that the correlation coefficient is significant at less than the 5% level)

Index	Superior	Huron	Michigan	Erie	Ontario
NAO	8/17	-1/0	-38/-32	-16/2	-29/-2
PNA	-9/-12	9/-25	11/-18	-18/-28	7/-39
TNH	32/65	33/58	39/74	31/47	25/46

absolute time series show similar but weaker correlation coefficients. The maps of the absolute time series correlations are not shown here for the sake of brevity). The teleconnection centres in Figure 5(a–e) are, in general, the same but are larger in areal extent than those identified in the anomaly difference map (Figure 4). Areas locally significant at the 5% confidence level have centres in the subtropical Pacific, Alaska, the Gulf of Alaska, Mexico east to the Gulf of Mexico, the vicinity of the Great Lakes, the mid-Atlantic Ocean (40°N, 40°W to 30°N, 60°W), Greenland, and western Europe and the adjacent Atlantic Ocean. Correlation coefficients in the Pacific Ocean are significant for three of the five Great Lakes (Superior, Huron, and Erie) and Alaskan centres are significant for all five Great Lakes, with the largest area of highest correlation coefficient for Lake Superior (Figure 5(a)). The correlation coefficients in the vicinity of the Great Lakes are significant for all the Great Lakes (Figure 5(a–e)). The Mexico centre has significant correlations for Lakes Superior, Huron, and Erie (Figure 5(a, c and d)). These four correlation centres (Pacific Ocean, Alaska, Great Lakes, and Mexico) appear to be somewhat similar in appearance to both distorted PNA and TNH teleconnection patterns. Lake Superior has the strongest, and Lake Ontario has the weakest correlation to these four centres.

Correlation coefficients in the western European centre are significant for Lakes Superior, Michigan, Huron, and Ontario (Figure 5(a, b, c and e)). The correlation maps for Lakes Michigan, Erie, and Ontario have an entire belt of negative correlation coefficients in the middle latitudes from 110°W to 40°E (Figure 5(b, d and e)); Lakes Michigan and Ontario maps also have a major area of positive correlation coefficients north of 50°N in the Atlantic and North America. This western Europe–North Atlantic pattern suggests a NAO-like teleconnection (not the classic NAO pattern) with annual maximum ice cover in Lakes Michigan, Ontario, and possibly Huron. A negative mode of the NAO appears to be associated with above average ice cover on the Great Lakes. The negative mode of the NAO pattern usually results in above normal temperature anomalies west of Greenland (van Loon and Rogers, 1978), however, it is colder than normal in the Great Lakes region. Alternatively, when the NAO mode is positive there are strong westerly winds in the mid-latitude belt and positive temperature anomalies in the Great Lakes region. As a result, ice cover in the Great Lakes, and particularly Lakes Michigan, Huron, and Ontario, tends to be below average with the positive NAO mode.

7. GREAT LAKES ICE COVER CORRELATIONS WITH PNA, NAO, AND TNH INDICES

Correlation coefficients between the teleconnection indices and maximum ice cover in the Great Lakes for both the original time series and their first difference time series are presented in Table VI. The only teleconnection index that significantly correlates with ice cover on all the lakes is the TNH index. It is particularly strong for Lake Michigan; as seen in Figure 6 the relationship between the first differences is almost functional. Despite the high correlation coefficient (0.74), however, the spatial characteristics of our pattern differ from those of the TNH. The most noticeable differences are the absences of the

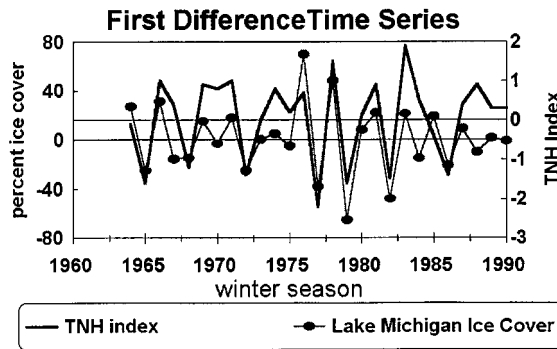


Figure 6. Lake Michigan ice cover and TNH index (first differences)

Caribbean anomaly centre on our maps and, alternatively, the presence of a central Pacific centre, which is an element of the PNA pattern.

The relative contribution of the NAO, PNA, and TNH teleconnection indices as well as their joint effect on Great Lakes ice cover was estimated by using multiple regression equations between the teleconnection indices and maximum ice cover. Computed coefficients of determination (adjusted by the number of degrees of freedom) show what percentage of variance in ice cover is explained by a linear combination of the three indices (Table VII). Calculations were made both for the absolute values and the first differences. Because there is no significant correlation between the teleconnection indices, and because they were normalized by their standard variation, regression coefficients in each of the equations serve as indicators of the relative importance of each of the indices. The percentage of variance in ice cover explained by a joint effect of all three patterns is negligible. Even for Lake Michigan, where the effect of the teleconnection indices reached the maximum, it explained less than a quarter of ice cover variance. This effect becomes significantly more pronounced for the first difference, particularly for Lakes Superior and Michigan, where it explains about half the ice cover variance.

8. SUMMARY AND CONCLUSIONS

Differences in lake heat storage and differences in latitude (41°N–40°N) are important local factors affecting the annual maximum ice cover of the Great Lakes. The Northern Hemisphere's upper air general circulation pattern, which controls the origin, frequency, and duration of winter air mass movements over the Great Lakes, is an important global factor affecting the Great Lakes ice cover, as evidence by teleconnections.

Table VII. Coefficient of determination (r^2) reflecting percentage of variance in Great Lakes annual maximum ice cover explained by a linear combination of the NAO, PNA, and TNH indices and relative contribution (%) of each of them. The first number is for absolute values and the second is for the first differences

Index	Superior	Huron	Michigan	Erie	Ontario
NAO	26/38	4/26	43/20	22/28	47/29
PNA	20/1	29/15	24/15	29/25	23/28
TNH	54/61	67/59	33/65	49/47	30/43
r^2 (%)	1/49	1/29	23/52	2/18	5/21

8.1. Changes in the annual maximum ice cover regime

There are two statistically significant changes in the ice cover regime relative to the 28-winter average: shift from below average (1963–1976) to above average (1977–1982) in 1977 and shift from above average to below average (1983–1990) in 1983. The six-winter above average ice cover regime was initiated by an interdecadal change in northern hemispheric circulation that started in 1977 and was accompanied by a five-winter hiatus in ENSO events, winters from 1978 to 1982.

8.2. ENSO and ice cover

The analysis given in this paper is only a first exploratory look at possible ENSO–Great Lakes ice cover teleconnections. A relatively strong tendency for below average ice cover (46% of the lowest quartile annual maximum ice) was found for year + 1 warm ENSO event winters. The data showed no similarly strong signal for highest quartile ice cover for La Niña ENSO events. Clearly more work is needed to further explore the relationship between ENSO and Great Lakes ice cover and the potential of ENSO as a long-range forecast predictor of Great Lakes ice cover.

8.3. Hemispheric circulation patterns and teleconnections

Composite anomaly maps of 700 hPa for the extreme winters show that winters of much-above average ice cover are representative of a meridional flow regime, and winters of much-below average ice cover occur with a zonal flow regime over North America. Anomaly difference maps (composite 700 hPa anomaly map for the high quartile ice cover winters minus composite 700 hPa anomaly map for the low quartile ice cover winters) and the composite anomaly maps themselves provide evidence of ice cover teleconnections. Correlations of first differences of annual maximum ice cover with first differences of mean winter 700 hPa geopotential heights over the 28 winters under study had significant correlations over the subtropical Pacific, Alaska, western Europe and adjacent Atlantic Ocean, and the Great Lakes. The significant first differences (high-pass filter) correlations imply strong interannual teleconnections and a possible connection with the Quasi-Biennial Oscillation.

8.4. Correlations with the PNA, NAO, and TNH teleconnections

A regression analysis of the standardized indices of the PNA, NAO, and TNH (Tables VI and VII) shows that only the TNH index is significantly correlated with ice cover on all five Great Lakes. Thus, the ice cover teleconnection pattern for each Great Lake, although unique, appears to be related to the TNH pattern. The TNH pattern along with the PNA pattern affects the strength and position of the ridge–trough system over North America. The positive phase of the TNH pattern, when the centre over the Great Lakes is anomalously deep, corresponds to a more meridional circulation over the continent, whereas during the negative phase the circulation is more zonal. The predominant position of these ridge and trough systems is shifted in a longitudinal direction compared with that for the PNA pattern.

8.5. Future work

Results given here are encouraging enough to further explore Great Lakes ice cover teleconnections for possible use in development of long-range forecasts of Great Lakes ice cover. Analysis of North Pacific SST anomalies in relation to winter upper air circulation characteristics over North America may provide the key to improved understanding of Great Lakes ice cover teleconnections. Wallace *et al.* (1990) found that the correlation map of simultaneous time series of the expansion coefficient of the first empirical orthogonal function (EOF) of North Pacific SST and hemispheric 500 hPa heights resembles the PNA pattern. Analogous calculations performed on the SST anomalies averaged from February through to April minus the SST anomalies averaged from October through to December of the previous calendar year with the corresponding 500 hPa pattern was almost spatially orthogonal to the PNA, with many features common with the TNH (and thus Great Lakes ice cover) teleconnection. The pattern of EOF 1

of the mid-winter SST difference is similar to EOF 1 of SST itself; both have a primary 'centre of action' of a positive sign surrounded by negative values of the loading vector. An SST distribution pattern of this kind is characteristic of winters with a cold ENSO event and is conducive to zonal circulation over North America. An opposite SST sign anomaly pattern is often observed during warm ENSO events and favours meridional circulation, an enhanced upper ridge over the West Coast (of North America), and a strong upper trough downstream. More subtle differences in SST anomalies may determine the position of the upper atmospheric ridge and trough over North America, what pattern, PNA or TNH, will dominate, and Great Lakes ice conditions.

ACKNOWLEDGEMENTS

This is Great Lakes Environmental Research Laboratory (GLERL) Contribution No. 1020. The authors are indebted to Lynn Herche and Brent Lofgren of GLERL for their review of the manuscript and to the two anonymous journal reviewers for their helpful comments and suggestions.

REFERENCES

- Assel, R.A. 1986a. 'The winter of 1985–86', *Lakes Lett.*, **17**(2).
- Assel, R.A. 1986b. *Great Lakes Degree-day and Winter Severity Index Update: 1897–1983*, NOAA Data Report ERL GLERL-29, Great Lakes Environmental Research Laboratory, Ann Arbor, MI, 54 pp.
- Assel, R.A. 1987. 'The winter of 1986–87', *Lakes Lett.*, **18**(2).
- Assel, R.A. 1989. 'Impact of global warming on Great Lakes ice cycles', in Smith, J.B. and Tirpak, D.A. (eds), *The Potential Effects of Global Climate Change on the United States*, US Environmental Protection Agency, EPA-230-05-89-051, Washington, DC.
- Assel, R.A. 1990. 'An ice cover climatology for Lake Erie and Lake Superior for the winter season 1897–1898 to 1982–1983', *Int. J. Climatol.*, **10**, 731–748.
- Assel, R.A. 1992. 'Great Lakes winter-weather 700-hPa PNA teleconnections', *Mon. Wea. Rev.*, **120**(9), 2156–2163.
- Assel, R.A. and Quinn, F.H. 1979. 'A historical perspective of the 1976–77 Lake Michigan ice cover', *Mon. Wea. Rev.*, **107**, 336–341.
- Assel, R.A. and Robertson, D.M. 1995. 'Changes in winter air temperatures near Lake Michigan during 1851–1993, as determined from regional lake-ice records', *Limnol. Ocean.*, **40**(1), 165–176.
- Assel, R.A., Boyce, D.E., DeWitt, B.H., Wartha, J.H. and Keyes, F.A. 1979. *Summary of Great Lakes Weather and Ice Conditions, Winter 1977–78*, NOAA Technical Memorandum ERL GLERL-26, Great Lakes Environmental Research Laboratory, Ann Arbor, MI.
- Assel, R.A., Snider, C.R. and Lawrence, R. 1985. 'Comparison of 1983 Great Lakes winter weather and ice conditions with previous years', *Mon. Wea. Rev.*, **113**, 291–303.
- Assel, R.A., Janowiak, J., Boyce, D. and Young, S. 1996. 'Comparison of 1994 Great Lakes winter weather and ice conditions with previous years', *Bull. Am. Meteorol. Soc.*, **77**(1), 71–88.
- Barnston, A.G. and Livezey, R.E. 1987. 'Classification, seasonality and persistence of low-frequency atmospheric circulation patterns', *Mon. Wea. Rev.*, **115**, 1083–1126.
- Brown, R., Taylor, W. and Assel, R.A. 1993. 'Factors affecting the recruitment of lake whitefish in two areas of northern Lake Michigan', *J. Great Lakes Res.*, **19**, 418–428.
- DeWitt, B.H., Kahlbaum, D.F., Baker, D.G., Wartha, J.H., Keys, F.A., Boyce, D.E., Quinn, F.H., Assel, R.A., Baker-Blocker, A. and Kurdziel, K.M. 1980. *Summary of Great Lakes Weather and Ice Conditions, Winter 1978–79*, NOAA Technical Memorandum ERL GLERL-31, Great Lakes Environmental Research Laboratory, Ann Arbor, MI.
- Dooley, H.D., Martin, J.H.A. and Ellett, D.J. 1984. 'Abnormal hydrographic conditions in the Northeast Atlantic during the 1970s', *Rapp. P. Reun. Cons. Int. Explor. Mer.*, **185**, 179–187.
- Graham, N.E. 1994. 'Decadal-scale climate variability in the tropical and North Pacific during the 1970s and 1980s: observations and mode results', *Climate Dyn.*, **10**, 135 pp.
- Hanson, P.H., Hanson, C.S. and Yoo, B.H. 1992. 'Recent Great Lakes ice trends', *Bull. Am. Meteorol. Soc.*, **73**, 577–584.
- Harnack, R.P. 1980. 'An appraisal of the circulation and temperature pattern for winter 1978–1979 and comparison with the previous two winters', *Mon. Wea. Rev.*, **108**, 37–55.
- Jenkins, G.M. and Watts, D.F. 1968. *Spectral Analysis and its Applications*, Holden-Day.
- Jenne, R.L. 1975. *Data Sets for Meteorological Research*, NCAR Technical Note TN-1A-111, 0, 194 pp.
- Kiladis, G.H. and Diaz, H.F. 1989. 'Global climatic anomalies associated with extremes in the Southern Oscillation', *J. Climate*, **2**, 1069–1090.
- Magnuson, J., Bowser, C., Assel, R.A., DeStasio, B., Eaton, J., Fee, E., Dillon, P., Mortsch, L., Routlet, N., Quinn, R. and Schindler, D. 1995. 'Region 1.—Laurentian Great Lakes and Precambrian Shield', in *Symposium Report, Regional Assessment of Freshwater Ecosystems and Climate Change in North America*, American Society of Limnology and Oceanography, and North American Benthological Society.
- Mo, K.C. and Livezey, R.E. 1986. 'Tropical–extratropical geopotential height teleconnections during the Northern Hemisphere winter', *Mon. Wea. Rev.*, **114**, 2488–2414.
- National Center for Atmospheric Research 1996. *National Meteorological Center Grid Point Data Set. CDROM: Version III. General Information and User's Guide*, Data Support Section, National Center for Atmospheric Research, Boulder, CO 80303.

- Niimi, A.J. 1982. 'Economic and environmental issues of the proposed extension of the winter navigation season and improvements on the Great Lakes-St. Lawrence Seaway system', *J. Great Lakes Res.*, **8**, 532–549.
- Quinn, F.H., Assel, R.A., Boyce, D.E., Leshkevich, G.A., Snider, C.R. and Weisnet, D. 1978. *Summary of Great Lakes Weather and Ice Conditions, Winter 1976–77*, NOAA Technical Memorandum ERL GLERL-20, Great Lakes Environmental Research Laboratory, Ann Arbor, MI.
- Rodionov, S.N. and Krovvin, A.S. 1992. 'The 1980s in the context of climate changes in the North Atlantic region', *ICES Mar. Sci. Symp.*, **195**, 86–95.
- Rogers, J.C. 1976. *Long-range Forecasting of Maximum Ice Extent on the Great Lakes*, NOAA Technical Memorandum ERL GLERL-7, Great Lakes Environmental Research Laboratory, Ann Arbor, MI.
- Ropelewski, C.F. and Halpert M.S. 1986. 'North America precipitation and temperature patterns associated with the El Niño/Southern Oscillation (ENSO)', *Mon. Wea. Rev.*, **114**, 2352–2362.
- Ryan, C.M., Quinn, F.H. and Donahue, M.J. 1994. *Proceedings of the Great Lakes Climate Change Workshop*, NOAA Cooperative Institute of Limnology and Ecosystems Research, University of Michigan, Ann Arbor, MI.
- Smith, J.B. 1991. 'The potential impacts of climate change on the Great Lakes', *Bull. Am. Meteorol. Soc.*, **72**, 21–28.
- Trenberth, K.E. 1990. 'Recent observed interdecadal climate changes in the Northern Hemisphere', *Bull. Am. Meteorol. Soc.*, **71**, 988–993.
- Vanderploeg, H.A., Bolsenga, S.J., Fahnenstiel, G.L., Liebig, J.R. and Gardner, W.S. 1992. 'Plankton ecology in an ice-covered bay of Lake Michigan: utilization of a winter phytoplankton bloom by reproducing copepods', *Hydrobiologia*, **243–244**, 175–183.
- van Loon, H. and Rogers, J.C. 1978. 'The seesaw in winter temperatures between Greenland and Northern Europe. Part I: General description', *Mon. Wea. Rev.*, **106**, 296–310.
- Wallace, J.M. and Gutzler, D.S. 1981. 'Teleconnections in the geopotential height field during the Northern Hemisphere winter', *Mon. Wea. Rev.*, **109**(4), 784–812.
- Wallace, J.M., Smith, C. and Jiang, Q. 1990. 'Spatial patterns of atmosphere–ocean interaction in the northern winter', *J. Climate*, **3**, 990–998.
- Wang, B. 1995. 'Interdecadal changes in El Niño onset in the last four decades', *J. Climate*, **8**, 267–285.